RAPID COMMUNICATIONS

PHYSICAL REVIEW B VOLUME 47, NUMBER 23 15 JUNE 1993-I

Observation of valence-band Landau-level mixing by resonant magnetotunneling

A. Zaslavsky, D. A. Grützmacher, S. Y. Lin, T. P. Smith III, R. A. Kiehl, and T. O. Sedgwick
IBM Research Division, Thomas J. Watson Research Center, Yorktown Heights, New York 10598
(Received 25 January 1993)

In magnetotunneling $I(V,B_{\|})$ measurements on strained p-type $Si/Si_{1-x}Ge_x$ double-barrier resonant tunneling structures we observe heavy-hole satellite peaks that correspond to tunneling with $\Delta n=1$ and 2 changes in the Landau index n. The relative intensity of the satellite peaks excludes scattering as a possible mechanism. We ascribe the $\Delta n=1,2$ satellites to elastic tunneling made possible by Landau-level mixing in the valence band predicted by the Luttinger Hamiltonian in a magnetic field. The satellite peak spacing yields the valence-band Landau-level structure in strained $Si_{1-x}Ge_x$ quantum wells.

Since the observation of Landau levels in a double-barrier resonant tunneling structure (DBRTS) by Mendez, Esaki, and Wang,[1] magnetotunneling has been commonly employed to study transport in these devices. If the tunneling carriers are described by a single parabolic band, like electrons in $GaAs/Al_xGa_{1-x}As$ DBRTS, the effect of a magnetic field B parallel to the current direction ($B\|I\|z$) is well understood. The electronic states in the plane transverse to the tunneling direction z are constrained into evenly spaced Landau levels of energy $E_n=\hbar\omega_c(n+\frac{1}{2})$ with corresponding in-plane harmonic-oscillator wave functions $\phi_n(r_{\perp})$. In a magnetic field, the energy E and transverse momentum $k_{\perp}$ conservation rules that govern tunneling from the three-dimensional (3D) emitter into the 2D well at $B_{\|}=0$ (Ref. 2) are transformed into the conservation of E and Landau index n.[1,3,4] As a result, the $I(V,B_{\|})$ resonant peak can acquire a weak staircaselike or sawtooth structure, with evenly spaced features corresponding to the successive alignment of Landau levels in the well and the emitter. Significantly, as long as the Landau index is conserved ($\Delta n=0$), the magnetic field cannot produce any structure in $I(V,B_{\|})$ at a bias higher than the resonant peak. A scattering process, like LO-phonon emission, can lead to the appearance of a phonon replica[5] exhibiting $\Delta n\neq 0$ tunneling features in a $B_{\|}$ field,[5,6] but the replica peak due to inelastic tunneling is invariably much weaker than the main resonant peak.

If the tunneling carriers cannot be described by a parabolic band, as in the case of p-type devices in $GaAs/Al_xGa_{1-x}As$ (Refs. 7 and 8) and $Si/Si_{1-x}Ge_x$ (Refs. 9 and 10), the effect of $B_{\|}$ is more complex (for theoretical treatment of hole DBRTS see Ref. 11). Since the hole states belong to interacting heavy-hole (HH) and light-hole (LH) bands with nonparabolic dispersion, there is no reason to expect evenly spaced Landau levels even in bulk material. The addition of strain or quantum-well interfaces complicates the situation further. Calculations of 2D hole Landau levels[12] reveal a complicated structure with strong nonlinearities and level crossings. Experimental measurement of hole Landau levels has relied primarily on magneto-optics and cyclotron resonance techniques in III-V heterostructures;[13] recently, cyclotron resonance measurements on holes in $Si/Si_{1-x}Ge_x$ quantum wells were reported.[14] Parallel field magnetotunneling in DBRTS should provide an alternative experimental technique, especially in indirect semiconductors like the scientifically and technologically interesting strained $Si/Si_{1-x}Ge_x$ system, but observation of Landau levels in $I(V,B_{\|})$ of p-type structures has proved elusive. There have only been reports of weak features in the derivative of the LH_0 current peak that were attributed to Landau index nonconserving ($\Delta n=1$) tunneling due to scattering.[15]

In our experiments we have studied three p-type $Si/Si_{1-x}Ge_x$ DBRTS samples, identical in design except for the $Si_{1-x}Ge_x$ well thickness W. These samples were grown on Si substrates by atmospheric pressure chemical-vapor deposition; the details of sample design, growth, and processing have been published elsewhere.[16] The active DBRTS region comprises 50-Å Si barriers cladding a $Si_{1-x}Ge_x$ well (Ge content $x=0.25$) with $W=23$, 35, or 46 Å. On either side of the active structure are undoped $Si_{1-x}Ge_x$ ($x=0.25$) spacer layers that are graded to heavily doped Si regions.[16] Consequently, the holes tunnel from a $Si_{1-x}Ge_x$ emitter into the $Si_{1-x}Ge_x$ well through a Si barrier. The strain in the $Si_{1-x}Ge_x$ layers splits the HH and LH valence-band edges by $\Delta\varepsilon\geq 40$ meV (Ref. 17) and at low temperatures only the HH states are occupied in the emitter (we follow the convention that "heavy-hole" and "light-hole" designations refer to the effective mass in the tunneling direction m_z^* at $k=0$). The band diagram of the emitter and 2D well subbands under bias together with a schematic of their in-plane dispersion $E(k_{\perp})$ for the $W=35$ Å structure is shown in Fig. 1(a), while the zero-field $I(V,B_{\|}=0)$ characteristics of the three samples are shown in Fig. 1(b). All three samples exhibit resonant peaks corresponding to holes tunneling from the emitter into the HH_0 and LH_0 2D hole subbands in the well [in the $W=46$ Å sample the HH_1 peak also falls in the bias range of Fig. 1(b)]. The peak-to-valley ratios are very high for p-type DBRTS, reaching 2:1 for HH_0 peaks and 4:1 for LH_0 peaks. A self-consistent calculation of the potential distribution over the device[18] was used to convert the applied bias V to the alignment of the occupied emitter states with the 2D subbands. The energies of the HH_i and LH_i subbands were calculated using the $m_z^*=(\gamma_1\pm 2\gamma_2)^{-1}$ values obtaining from a linear interpo-

lation of Si and Ge valence-band parameters. Since the quantum-well confinement adds to the strain-induced splitting of the HH_0 and LH_0 bands, the in-plane dispersion of the HH_0 band is nearly parabolic on the scale of emitter Fermi energy $E_F \sim 10$ meV. Hence, in the envelope-function approximation, the expected bias positions of the threshold V_{th} and peak V_p of the HH_0 resonance can be easily determined from E and $k_\perp$ conservation:[2] V_{th} occurs when the HH_0 subband aligns with E_F in the emitter, V_p occurs when HH_0 approximately aligns with the top of the emitter valence band [see Fig. 1(a)]. The agreement between the calculated position of the HH_0 peak and the experimental data for all three samples is shown in Fig. 1(b). The in-plane dispersion of the LH_0 subband is strongly nonparabolic and can become electronlike in the presence of a nearby HH_1 band.[19] Consequently, the comparison of LH_0 peak positions with experiment in the $(E,k_\perp)$ conservation framework requires numerical calculation of these subbands, which will be reported separately. Here we focus on the surprising magnetotunneling characteristics $I(V,B_\parallel)$ of the HH_0 peaks.

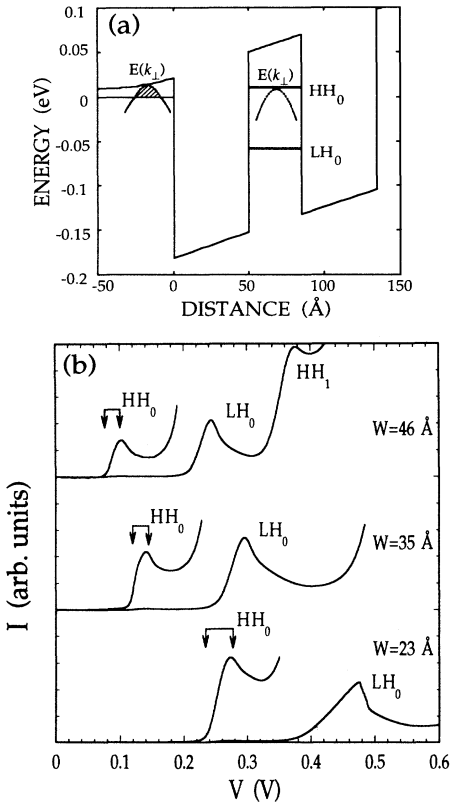

FIG. 1. (a) Calculated potential distribution of the double-barrier resonant tunneling structure with well width $W=35$ Å under bias $V=140$ mV, together with schematic $E(k_\perp)$ dispersion in the emitter HH band and the HH_0 2D subband in the well (occupied emitter states are hatched). (b) Tunneling $I(V)$ characteristics at $T=42$ K and $B_\parallel=0$ of structures with $W=23$, 35, and 46 Å, together with expanded (50×) views of the HH_0 peaks. Resonant current peaks correspond to tunneling through the labeled 2D subbands. Arrows show the calculated threshold and peak bias values for the HH_0 peaks.

The $I(V,B_\parallel)$ characteristics of the HH_0 peak in the $W=35$ Å DBRTS at $B_\parallel=7.5$, 15, 20, and 30 T are shown in Fig. 2. The low-field $B_\parallel=7.5$ T trace is nearly identical to the zero-field data of Fig. 1(b), except for a weak shoulder appearing ~30 mV above the main HH_0 peak ($V_p=140$ mV). As $B_\parallel$ increases, the main peak remains nearly unchanged in position and becomes gradually weaker. The shoulder grows into a satellite peak that moves to higher bias with $B_\parallel$, becomes comparable in magnitude to the main peak at $B_\parallel \sim 15$ T, and dominates at $B_\parallel=30$ T where the splitting between the two reaches ~90 mV. Furthermore, at $B_\parallel \geq 20$ T another, weaker satellite feature appears between the main peak and the satellite. This feature also moves to higher bias with $B_\parallel$ and gains in strength, although it never becomes comparable to the main peak (see Fig. 2).

Samples with $W=23$ and 46 Å, measured up to $B_\parallel=11$ T, exhibit analogous behavior to the $W=35$ Å device of Fig. 2: a satellite peak appears at $B_\parallel \sim 7$ T, moves to higher bias and becomes stronger with $B_\parallel$, while the main peak does not shift appreciably. The main and satellite peak positions of the HH_0 line shape in all three samples is shown in Fig. 3. From the $B_\parallel$-induced shifts in satellite peak positions, we attribute the stronger satellite to $\Delta n=2$ tunneling (from $n=0$ in the emitter to $n=2$ in the well) and the weaker satellite to $\Delta n=1$ tunneling ($n=0$ to $n=1$). In all samples, at low $B_\parallel$ the main $\Delta n=2$ satellite shifts nearly linearly with $B_\parallel$ with the same slope of ~3.5 mV/T. At high $B_\parallel$ in the $W=35$ Å structure, where the $\Delta n=2$ satellite peak position $V_p^{\Delta n=2} \geq 220$ mV, the slope begins to decrease. The weaker $\Delta n=1$ satellite shifts linearly with $B_\parallel$ up to 30 T, the highest field measured. The absence of additional $B_\parallel$-induced steplike structure in the main peak[1,4] is due to the fact that at $B_\parallel$ fields sufficient to resolve adjacent Landau levels (see Fig. 2) the occupied emitter states are

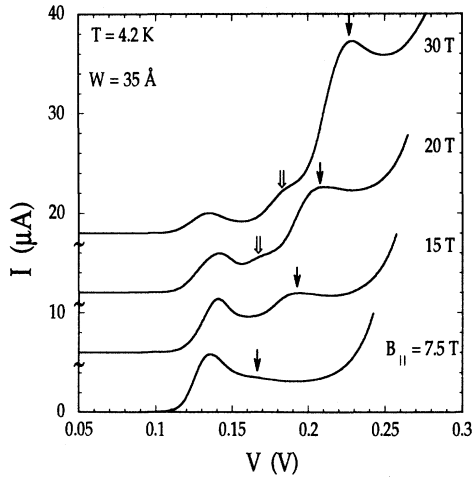

FIG. 2. $I(V,B_\parallel)$ characteristics of the $W=35$ Å structure at $B_\parallel=7.5$, 15, 20, and 30 T. The curves have been displaced by 6 μA for clarity. The positions of satellite peaks corresponding to Landau index n nonconserving tunneling are indicated by solid ($\Delta n=2$) and open ($\Delta n=1$) arrows.

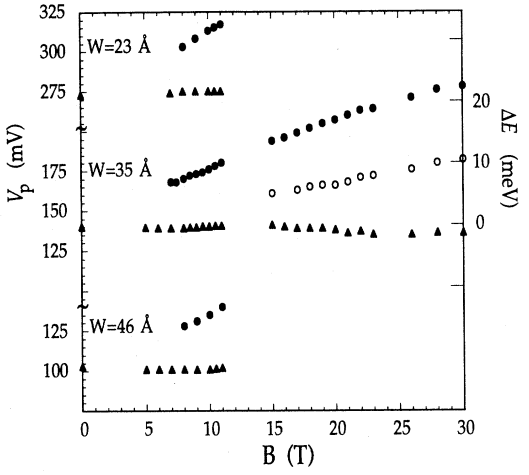

FIG. 3. Bias positions of the main ($\Delta n=0$, triangles) and satellite ($\Delta n=1$, open circles; $\Delta n=2$, filled circles) peaks as a function of $B_\parallel$. The scale on the right corresponds to the calculated energy scale of the Landau-level structure in the $W=35$ Å device; the zero of energy is arbitrarily chosen to coincide with the main peak position at $B_\parallel=0$.

all in the lowest $n=0$ Landau level.

The strength of the $\Delta n=2$ satellite, which becomes comparable to the main peak at moderate $B_\parallel$ and increases with $B_\parallel$, together with the relative weakness of the $\Delta n=1$ satellite indicate clearly that these $I(V,B_\parallel)$ resonances cannot arise via a scattering mechanism. Although interface and impurity scattering can relax $k_\perp$ conservation or, equivalently, Landau index n conservation,[15] these mechanisms are unlikely to produce satellite peaks comparable in strength to the main, index-conserving peak. Moreover, the $\Delta n=1$ satellite is much weaker than $\Delta n=2$, although the required change in transverse momentum in the $\Delta n=2$ case is much larger if the satellites are attributed to scattering. Taking the tunneling barrier reduction with applied bias into account does not alter the discrepancy in the relative strength of the satellite peaks: as Fig. 2 shows, when $B_\parallel=30$ T the $\Delta n=1$ peak occurs at $V\sim 180$ mV and is much weaker than the $\Delta n=2$ peak that occurs at $V>180$ mV when $B_\parallel=15$ T. Thus, instead of attributing the appearance of satellite peaks to scattering-assisted tunneling, we qualitatively interpret our results within the Luttinger analysis of the valence band in a magnetic field[20–22] to demonstrate that valence-band Landau-level mixing allows index-nonconserving ($\Delta n\neq 0$) tunneling that does not require scattering.

Since we are dealing with magnetotunneling from the occupied heavy-hole Landau-level states in the emitter into the Landau levels of the HH_0 2D subband, the problem is described by the effective 4×4 Hamiltonian H_{ij} in the $|Jm_j\rangle$ basis: $J=\frac{3}{2}$, the quantization axis is $z\|B_\parallel$, and $i,j=1,2,3,4$ label the states $m_j=\frac{3}{2},\frac{1}{2},-\frac{1}{2},-\frac{3}{2}$ in that order. For bulk bands and no strain H_{ij} was derived by Luttinger;[20] uniaxial strain contributes only to diagonal elements H_{ii} and splits the $|\frac{3}{2}\pm\frac{3}{2}\rangle$ (HH) and $|\frac{3}{2}\pm\frac{1}{2}\rangle$ (LH) bands by $\Delta\varepsilon$.[17,21] In a magnetic field, all H_{ij} elements can be expressed in terms of harmonic-oscillator raising and lowering operators a and a_+; consequently the four-component Landau-level eigenfunctions Ψ_n can be written as a superposition of harmonic-oscillator wave functions $\phi_n(r_\perp)$:[20,22]

$$\Psi_n^{l,h}=[\zeta_{1,n}\phi_{n-2};\zeta_{2,n}\phi_{n-1};\zeta_{3,n}\phi_n;\zeta_{4,n}\phi_{n+1}]\ , \tag{1}$$

where $\zeta_{i,n}(z)$ are linear combinations of products $c_i(z)|Jm_j\rangle$, with $c_i(z)$ determined by the boundary conditions on Ψ_n [for terms in (1) that would have a negative oscillator index, $c_i(z)\equiv 0$]. The diagonal H_{ii} terms in the Luttinger Hamiltonian are of the form $(aa_+ +\frac{1}{2})$ and hence would give rise to separate sets of heavy- and light-hole Landau levels with linear $B_\parallel$ dependence, while the off-diagonal terms cause Landau-level mixing, leading to nonlinear $B_\parallel$ dependence and uneven level spacing.[22]

Given certain approximations, the wave functions $\Psi_n^{l,h}$ of (1) and the corresponding Landau-level energies can be solved analytically.[20] For example, in a bulk crystal with cylindrical symmetry (the in-plane anisotropy is neglected by setting Luttinger parameters $\gamma_2=\gamma_3=\bar{\gamma}$), at $k_z=0$ the only surviving off-diagonal H_{ij} elements are $H_{13}\sim a^2$, $H_{31}\sim a_+^2$. The wave function of the nth HH Landau level becomes[21]

$$\Psi_n^h=\phi_n|m_j=\tfrac{3}{2}\rangle-\alpha_{n+2}\phi_{n+2}|m_j=-\tfrac{1}{2}\rangle\ , \tag{2}$$

where α_{n+2} is a numerical factor. Therefore, Landau levels with indices differing by $\Delta n=2$ have oscillator wave functions $\phi_n(r_\perp)$ in common. In a bulk crystal the common ϕ_n of different Landau levels in (1) are multiplied by different orthogonal $|m_j\rangle$ functions, as in Eq. (2), and n remains a constant of motion, but in the well and emitter regions of a DBRTS the $\zeta_{i,n}$ functions of Eq. (1) become linear combinations of $|m_j\rangle$ because of the boundary conditions at the barrier interfaces[22] and elastic tunneling between Landau levels with $\Delta n=2$ is allowed. Hence the strong $\Delta n=2$ satellite peak in the $I(V,B_\parallel)$ shown in Fig. 2: the Ψ_0 wave function of the $n=0$ Landau level in the emitter (which contains all the occupied states at high $B_\parallel$) and the Ψ_2 wave function of the $n=2$ Landau level of the HH_0 subband in the well are nonorthogonal in the plane, leading to elastic tunneling that need not conserve n.

Analogously, when $k_z\neq 0$ another pair of off-diagonal terms in the Luttinger Hamiltonian $H_{12}\sim k_z a$, $H_{21}\sim k_z a_+$ (Refs. 20 and 22) describe the mixing of oscillator functions ϕ_n and ϕ_{n-1} in the total wave function Ψ_n of Eq. (1), allowing $\Delta n=1$ elastic tunneling. From the relative strength of the satellite peaks in Fig. 2, we find that the mixing of Landau levels with $\Delta n=1$ is about an order of magnitude weaker than of levels with $\Delta n=2$. This appears qualitatively consistent with the magnitude of the relevant H_{ij} terms in the Hamiltonian, since the $I(V)$ resonant peaks occur when the 2D subbands in the well are nearly aligned with the bottom of the band in the emitter, where k_z of the tunneling holes is small.[2] A quantitative description of the satellite peak magnitudes as a function of $B_\parallel$ requires a numerical calculation of the functions $\zeta_{i,n}$ in Eq. (1), in principle similar to the calculation of HH-LH band mixing away from $k=0$ by An-

dreani, Pasquarello, and Bassani.[23]

The $I(V,B_{\|})$ structure does not reflect the absolute Landau-level energies since the levels move together in the emitter and well, leaving the index-conserving main peak at approximately constant bias. On the other hand, the difference in energy between Landau levels $n=0,1,2$ can be determined from the $I(V,B_{\|})$ characteristics by converting the bias scale of Fig. 2 into an energy scale, i.e., by calculating self-consistently the fraction α of the total bias V that contributes to the alignment $\Delta E=\alpha V$ of the 2D levels in the well with the occupied emitter states.[3,4] In our samples the Si electrode layers outside the $Si_{1-x}Ge_x$ spacers are heavily doped and the depletion does not extend significantly past the $Si_{1-x}Ge_x$ spacer of the collector. As a result, for the bias range of interest in Fig. 2, α is well approximated by a constant: the energy scale ΔE obtained from the self-consistent calculation of the $W=35$ Å structure is shown on the right of Fig. 3. At low and moderate $B_{\|}$ the $\Delta n=2$ peak shifts linearly with $B_{\|}$ in all samples, indicating that the band is reasonably parabolic and hence the energy spacing between Landau levels can be taken as the measure of in-plane mass $m_{\|}^*$. From the self-consistent calculation we obtain a heavy-hole mass $m_{\|}^*=0.29\pm0.04$, considerably heavier than predicted by interpolating the Luttinger parameters for Si and Ge,[15] but in accord with the recent cyclotron resonance measurements.[14]

In conclusion, we have experimentally observed satellite peaks in the $I(V,B_{\|})$ characteristics of $Si/Si_{1-x}Ge_x$ DBRTS corresponding to tunneling between Landau levels that violates index conservation but cannot be attributed to scattering. We explain these index-nonconserving peaks within the Luttinger description of 2D Landau levels in DBRTS. Our experiments provide evidence of resonant tunneling processes that do not conserve Landau index and yet are allowed by the selection rules even in the absence of scattering. The data provide an experimental means of mapping out Landau levels in the valence band of strained $Si_{1-x}Ge_x$ quantum wells and other indirect-gap semiconductors, where cyclotron resonance and magneto-optics measurements are difficult.

We are pleased to acknowledge the assistance of the Francis Bitter National Magnet Lab staff and D. Syphers, as well as discussions with Dr. George Wu, Dr. E. E. Mendez, and Dr. F. Stern. Work at IBM was partially supported by ONR (Grant No. N0001492-C-0017).

[1]E. E. Mendez, L. Esaki, and W. I. Wang, Phys. Rev. B **33**, 2893 (1986).

[2]S. Luryi, Appl. Phys. Lett. **47**, 490 (1985).

[3]V. J. Goldman, D. C. Tsui, and J. E. Cunningham, Phys. Rev. B **35**, 9387 (1987).

[4]A. Zaslavsky, D. C. Tsui, M. Santos, and M. Shayegan, Phys. Rev. B **40**, 9829 (1989).

[5]V. J. Goldman, D. C. Tsui, and J. E. Cunningham, Phys. Rev. B **36**, 7635 (1987).

[6]M. L. Leadbeater, E. S. Alves, L. Eaves, M. Henini, O. H. Hughes, A. Celeste, J. C. Portal, G. Hill, and A. Pate, Phys. Rev. B **39**, 3438 (1989).

[7]E. E. Mendez, W. I. Wang, B. Ricco, and L. Esaki, Appl. Phys. Lett. **47**, 415 (1985).

[8]R. K. Hayden, L. Eaves, M. Henini, D. K. Maude, J. C. Portal, and G. Hill, Appl. Phys. Lett. **60**, 1474 (1992).

[9]H. C. Liu, D. Landheer, M. Buchanan, and D. C. Houghton, Appl. Phys. Lett. **52**, 1809 (1988); H. C. Liu *et al.*, Superlatt. Microstruct. **5**, 213 (1989).

[10]K. L. Wang, J. Park, S. S. Rhee, R. P. Karunasiri, and C. H. Chern, Superlatt. Microstruct. **5**, 201 (1989).

[11]R. Wessel and M. Altarelli, Phys. Rev. B **40**, 12 457 (1989).

[12]U. Ekenberg and M. Altarelli, Phys. Rev. B **32**, 3712 (1985).

[13]F. Ancilotto, A. Fasolino, and J. C. Maan, Superlatt. Microstruct. **3**, 187 (1987), and references therein.

[14]J.-P. Cheng, V. P. Kesan, D. A. Grützmacher, and T. O. Sedgwick, Appl. Phys. Lett. **62**, 1522 (1993); V. P. Kesan (private communication).

[15]G. Schuberth, G. Abstreiter, E. Gornik, F. Schäffler, and J. F. Luy, Phys. Rev. B **43**, 2280 (1991).

[16]A. Zaslavsky, D. A. Grützmacher, Y. H. Lee, W. Ziegler, and T. O. Sedgwick, Appl. Phys. Lett. **61**, 2872 (1992), and references therein.

[17]R. People, Phys. Rev. B **32**, 1405 (1985).

[18]This calculation, using the HETMOD program courtesy of A. C. Warren (IBM Research), ignores the dynamically stored hole density in the well, which is negligible in symmetrically designed DBRTS (Ref. 4).

[19]E. P. O'Reilly and G. P. Witchlow, Phys. Rev. B **34**, 6030 (1986).

[20]J. M. Luttinger, Phys. Rev. **102**, 1030 (1956).

[21]G. E. Gurgenishvili, Fiz. Tverd. Tela Leningrad **5**, 2070 (1963) [Sov. Phys. Solid State **5**, 1510 (1964)]; G. R. Khutsishvili, *ibid.* **4**, 2708 (1962) [**4**, 1986 (1963)].

[22]D. A. Broido and L. J. Sham, Phys. Rev. B **31**, 888 (1985); L. J. Sham, in *High Magnetic Fields in Semiconductor Physics,* edited by G. Landwehr (Springer-Verlag, New York, 1987), pp. 288–294.

[23]L. C. Andreani, A. Pasquarello, and F. Bassani, Phys. Rev. B **36**, 5887 (1987).